Time-Dependent Close-Coupling Calculations of Dielectronic Capture in He

D. M. Mitnik and D. C. Griffin
Department of Physics, Rollins College, Winter Park, Florida 32789

M. S. Pindzola
Department of Physics, Auburn University, Auburn, Alabama 36849
(Received 27 November 2001; published 15 April 2002)

We report on the first time-dependent close-coupling calculation of dielectronic capture into a doubly excited state of a two-electron atom. An incoming electron is represented by a Gaussian wave packet which collides with singly ionized helium in its ground state. The close-coupling equations describe the propagation of the total compound wave function on a two-dimensional radial lattice. By projecting this wave function onto a doubly excited state of neutral helium, we can determine the probability amplitude for dielectronic capture into one of these states and the subsequent autoionization from it.

DOI: 10.1103/PhysRevLett.88.173004 PACS numbers: 32.80.Dz, 31.70.Hq

Revolutionary advances in experimental techniques and theoretical methods along with spectacular increases in computer power now provide opportunities for the development of a much more profound understanding of the atomic few-body problem. In recent years, a number of quantal nonperturbative methods have been developed which provide benchmark accuracy for electron-impact ionization of simple atoms and their ions [1–4]. Of particular interest are cases in which the incident electron has an energy equal to an autoionization resonance. It is then impossible to distinguish electrons that have been ejected directly from the atom from those that are first excited to an autoionizing level and subsequently ejected. As a result, these two processes will interfere and interference can be sensitive to physical effects not present in the $(e, 2e)$ process far from resonance [5,6]. This problem has been largely investigated by using perturbative methods (see, for example [7] and references therein). However, due to the delicate interplay between three-body effects in the incident channel and postcollisional Coulombic interactions between the three free particles in the final state, a fully quantal treatment of this problem is needed. Examples of the difficulties arising in a nonperturbative calculation of breakup processes through resonant states have been pointed out in the model calculations (involving only short-range interactions) in Ref. [8].

Among the fully quantal nonperturbative theories, the time-dependent close-coupling (TDCC) method has been successfully employed for calculations of electron-impact ionization [9–11]. However, before undertaking a TDCC calculation of the resonant contributions to ionization, further work is needed in order to learn how to treat resonance problems within this theoretical framework. It is in this spirit that we have undertaken the study of dielectronic capture into doubly excited resonances that, after autoionization, contribute to elastic scattering. This requires the development of methods for generating accurate wave functions for doubly excited autoionizing states and time-dependent close-coupling calculations of the capture and the subsequent decay of autoionizing states.

In this work, we study dielectronic capture and autoionization in two-electron systems by the direct solution of the time-dependent close-coupling equations. In this Letter we will present only results for capture into the $2s^2\,{}^1S$ autoionizing state of neutral He. For an electron colliding with a He^+ ion, the target electron is initially described by the radial wave function ϕ_{1s} obtained from the diagonalization of the one-electron Hamiltonian on the radial grid. The projectile electron at an initial time t_0, with an energy E_i and a momentum $k_i = \sqrt{2E_i}$, is represented in coordinate space by a Gaussian wave packet of width w, centered at a position s sufficiently far from the target electron,

$$g_{k_i}(r) = \frac{1}{(w^2\pi)^{1/4}}\, e^{-[(r-s)^2]/(2w^2)} e^{-ik_i r}. \qquad (1)$$

The corresponding width in momentum space is $\Delta k = 1/w$, thus the k-dependent energy width is $\Delta E = k_i \Delta k = k_i/w$.

The time-dependent wave function for a given LS symmetry is expanded in coupled spherical harmonics:

$$\Psi^{LS}(\vec{r}_1, \vec{r}_2, t) = \frac{1}{r_1 r_2} \sum_{\ell_1,\ell_2} P^{LS}_{\ell_1,\ell_2}(r_1, r_2, t) Y^{L}_{\ell_1,\ell_2}(\hat{r}_1, \hat{r}_2), \qquad (2)$$

where $P^{LS}_{\ell_1,\ell_2}(r_1, r_2, t)$ are two-electron radial wave functions and $Y^{L}_{\ell_1,\ell_2}(\hat{r}_1, \hat{r}_2)$ are the coupled spherical harmonics. Upon substitution of Eq. (2) into the time-dependent Schrödinger equation, we obtain the TDCC equations for each LS symmetry. We found that two coupled channels ($\ell_1\ell_2 = ss, pp$) are sufficient to obtain correlated ${}^1S$ functions for He, since the dd channel gives a very small contribution.

For the ${}^1S$ symmetry, we start with an initial radial wave function of the form

$$P_{00}^{00}(r_1, r_2, t_0) = \sqrt{\frac{1}{2}}\,[\phi_{1s}(r_1) \times g_k(r_2) + \phi_{1s}(r_2) \times g_k(r_1)]. \quad (3)$$

The formal expression for propagating the wave function over one time increment Δt is

$$\Psi(\vec{r}_1, \vec{r}_2, t + \Delta t) = e^{-iH\Delta t}\Psi(\vec{r}_1, \vec{r}_2, t). \quad (4)$$

This compound wave function is allowed to evolve in time using the numerical procedures described in previous TDCC papers (see, for example, Refs. [9,10]). The resulting two-electron wave function fully describes the correlation between the incoming and the target electron for all times following the collision.

The probability amplitude for dielectronic capture into a doubly excited state Φ at time t is determined from the total wave function using the projection

$$C_\Phi(t) = |\langle\Phi(\vec{r}_1, \vec{r}_2, t_0)|\Psi(\vec{r}_1, \vec{r}_2, t)\rangle|. \quad (5)$$

In order to determine this capture amplitude, we must generate the doubly excited states on a numerical lattice. The energies and wave functions of the He atom are calculated by relaxation of the initial wave function (a simple product of one-electron wave functions) in imaginary time $\tau = it$:

$$\frac{\partial\Phi(\vec{r}_1, \vec{r}_2, \tau)}{\partial\tau} = -H\Phi(\vec{r}_1, \vec{r}_2, \tau). \quad (6)$$

With no constraints, this imaginary time propagation will relax to the solution with the smallest eigenvalue of H, thus, after many iterations (renormalizing the wave function continuously), only the ground-level eigenfunction will survive. Higher energy eigenfunctions can be determined by imposing constraints during the iteration that require the desired states to be orthogonal to all lower states. Although this procedure has been used for calculation of the the low-lying singly excited states (e.g., $1snl$), it does not work for the calculation of the doubly excited states. However, the doubly excited, autoionization states may be determined by imposing an additional constraint on the relaxation that projects out the one-electron components of the lower-energy wave functions.

For a numerical grid having a mesh spacing $\Delta r = 0.2$ a.u., the energies of the doubly excited ^1S states obtained using this modified relaxation technique are within a few percent of the accepted values. These results can be improved significantly by using a finer radial mesh. However, our purpose here is to study the dynamics of capture into a doubly excited state, rather than obtain the most accurate values for the energies of these states. Examples of the wave functions obtained with this damped relaxation method are given in Fig. 1. The figure shows the total probability $|\Phi|^2$, for the $1s^2$, $2s^2$, $2s3s$, and $2p^2$ wave functions (for brevity, we will drop the ^1S specification in every state).

The results of our TDCC calculations of the probability amplitude for dielectronic capture [Eq. (5)] into $2s^2$ at the resonance energy ($E_i = \epsilon_{2s^2} - \epsilon_{1s} = 31.6$ eV) are presented in Fig. 2. The different curves are obtained with

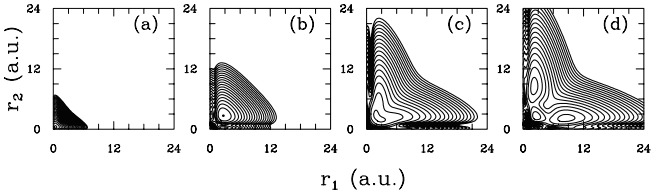

FIG. 1. TDCC wave functions obtained with the constrained damped relaxation method: (a) $1s^2$; (b) $2s^2$; (c) $2s3s$; (d) $2p^2$.

different initial wave packets, having spatial widths w of 5, 10, 15, and 30 a.u. ($\Delta E = 8.2$, 4.2, 2.8, and 1.4 eV), respectively. In this figure, $t = 0$ corresponds to the time when the center of the incoming wave packets arrives at the origin.

We see that the probability amplitude C_{2s^2} rises rapidly as the incoming wave packet begins to overlap with the target, with a slope that increases inversely with the width w of the incoming packet. After C_{2s^2} reaches a maximum, it begins a gradual decline with a slope that is a direct measure of the rate for autoionization from the $2s^2$ state to the ϕ_{1s} ground state of He^+.

The dynamical behavior of autoionization in two-electron systems has been studied previously by monitoring the decay of the autoionizing state Φ in time [12]. This requires the computation of the autocorrelation function defined by

$$A_\Phi(t) = |\langle\Phi(\vec{r}_1, \vec{r}_2, t_0)|\Phi(\vec{r}_1, \vec{r}_2, t)\rangle|, \quad (7)$$

where $\Phi(\vec{r}_1, \vec{r}_2, t)$ represents the initial wave function evolved in time. This method has been used to study autoionization in a one-dimensional two-electron model [13], a two-dimensional two-electron model [12], and an s-wave model [12,14].

By extending the autocorrelation method to include the ss and pp channels, we can compare the decay of the

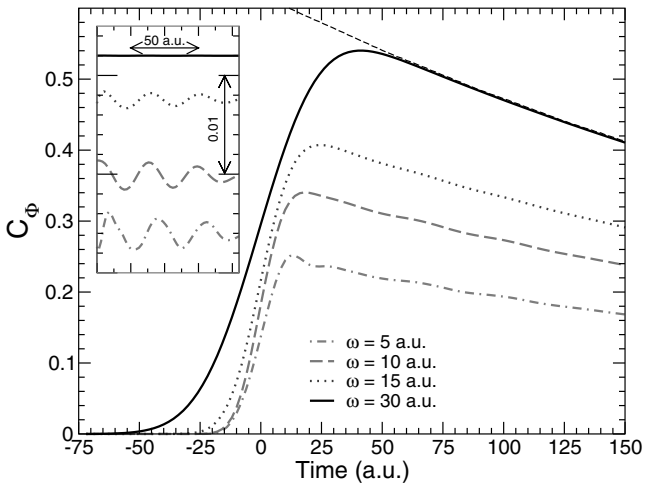

FIG. 2. TDCC amplitudes $C_\Phi(t) = C_{2s^2}(t)$ at resonance energy ($E_i = 31.6$ eV). The incoming wave packet has different spatial widths w from 5 to 30 a.u. The thin dashed line is the (scaled) A_{2s^2}. The inset shows the oscillations of the amplitudes around the asymptotic exponential decay (notice the different scale).

$2s^2$ state obtained from the autocorrelation method with the decay of the $2s^2$ state following dielectronic capture. The TDCC result for $A_{2s^2}(t)$ is also shown in Fig. 2 by the thin dashed line along the $C_{2s^2}(t)$ curve with a width of 30 a.u. In order to compare these two curves, we multiplied $A_{2s^2}(t)$ with $C_{2s^2}(t)$ at $t = 0$. As is shown in the figure, the agreement between the two calculations is excellent. An exponential fit of the form $\exp(-\frac{\Gamma}{2}t)$ to the data yields a value of $\Gamma_{2s^2} = 5.4 \times 10^{-3}$ a.u., compared to the width determined by Bhatia and Temkin [15] of 4.6×10^{-3} a.u. Our result can be improved by using a finer radial mesh. To confirm this, we repeated both the $C_{2s^2}(t)$ and $A_{2s^2}(t)$ calculations with $w = 30$ a.u., using a mesh separation of $\Delta r = 0.1$ a.u. An autoionization width of 4.9×10^{-3} a.u. was obtained from both curves.

A careful examination of the $C_{2s^2}(t)$ curves with different widths indicates that there are oscillations with small amplitudes in the decay of the autoionizing state. This is shown more clearly in the inset in Fig. 2. This effect is most pronounced for the curve corresponding to an initial wave packet with $w = 5$ a.u. ($\Delta E = 8.2$ eV). In energy space, this packet is sufficiently wide to coherently populate both the $2s^2$ and the $2s3s$ states (separated by 4.56 eV); these two states both autoionize to a single continuum state and this produces the observed beating. The period of these oscillations is about $T = 37.3$ a.u., corresponding to $\omega = \frac{2\pi}{T} = 4.6$ eV, confirming the origin of these oscillations. A similar effect has been observed in the calculation of intense field photoionization of He, in which two autoionizing states are populated by a broad laser pulse [16]. As expected, the oscillations decrease in amplitude as the energy width of the packets decreases and are completely absent for $w = 30$ a.u.

In order to obtain a quantitative measure in the variation of the capture probability with energy, we calculated the dielectronic capture for incoming wave packets with $w = 30$ a.u. at different incident energies, and some examples are presented in Fig. 3 (solid lines). We notice that the projection of the total wave function on the $2s^2$ state gives an unusually high overlap at energies far from resonance. This overlap rises and then falls off rapidly as the wave packet moves out beyond those radii where the $2s^2$ has any appreciable amplitude. The capture amplitude then falls off exponentially at the characteristic rate determined by the autoionizing width.

In order to gain an understanding of the shape of these curves, we employed a simple analytic one-dimensional model based on the perturbative approach for a discrete state $\phi(r)$ interacting with a single continuum state $\chi(r)$, as developed by Fano [17]. The eigenfunction of the Hamiltonian matrix for eigenvalue ϵ has the form

$$\Theta(\epsilon, r) = a(\epsilon)\phi(r) + \chi_\epsilon(r). \tag{8}$$

The function $|a(\epsilon)|^2$ has a Lorentzian shape centered at the resonance energy [17]. We construct the time dependent wave function

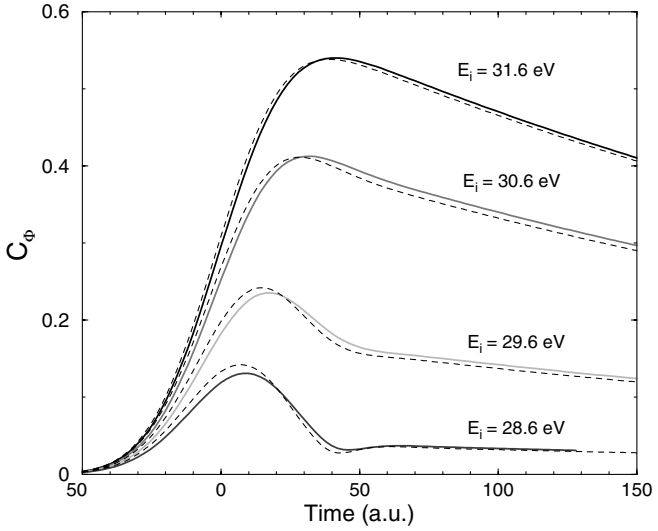

FIG. 3. TDCC amplitudes for $C_\Phi(t) = C_{2s^2}(t)$ at different incident energies. Thin dashed lines: perturbative calculations.

$$\Theta(t, r) = \int A(\epsilon)\Theta(\epsilon, r)e^{-i\epsilon(t-t_0)}\, d\epsilon\,, \tag{9}$$

where the function $A(\epsilon)$ is calculated from the initial conditions

$$A(\epsilon) = \int \Theta(\epsilon, r)\Theta(t_0, r)\, dr = \int \Theta(\epsilon, r) g_{k_i}(r)\, dr\,. \tag{10}$$

The perturbative dielectronic capture amplitude $D_\Phi(t)$ can then be obtained by projecting the $\Theta(t, r)$ function on to the resonance state $\phi(r)$:

$$D_\Phi(t) = |\langle\phi(r)|\Theta(t, r)\rangle| = \left| \int A(\epsilon)a(\epsilon)e^{-i\epsilon(t-t_0)}\, d\epsilon \right|. \tag{11}$$

We calculated $D_\Phi(t)$ for different incident electron energies, using the values of Γ_Φ and ϵ_Φ determined from the TDCC calculations. These results are also displayed in Fig. 3 by thin dashed lines; as can be seen, they are in very good agreement with the TDCC results. According to Eq. (11), at energies far from resonance, the long tail of $a(\epsilon)$ contributes to the integral (11) with a small and roughly constant value. By moving this constant outside the integral, the remaining equation represents the Fourier transform of the Gaussian function $A(\epsilon)$, which is itself a Gaussian; for energies far off resonance, this then explains the shape of the capture amplitude as a function of time.

The curves of $C_\Phi(t)$ at different energies allow us to perform fits at times where the decay is clearly exponential. Using these exponential fits, the curves were extrapolated back to $t = 0$, and the resulting probability amplitudes were employed to calculate maximum probabilities for capture into the $2s^2$ state. The curve of the maximum probability as a function of the incident energy is in agreement with the Fourier transform of a Gaussian

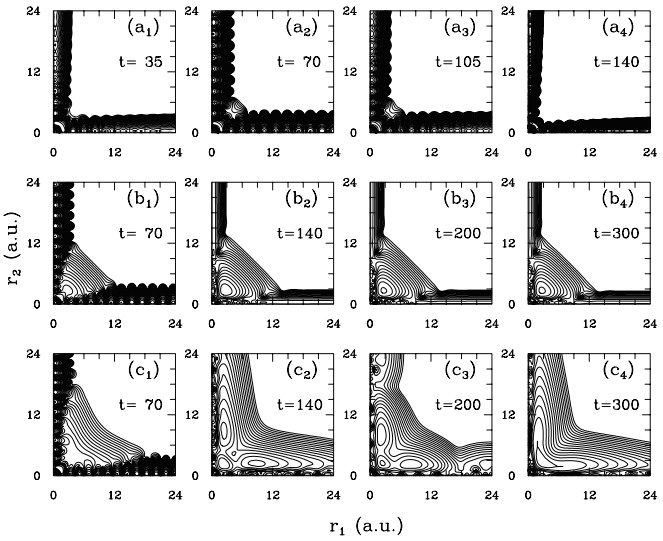

FIG. 4. Snapshots of the total wave function probability $|\Psi(r_1, r_2, t)|^2$ at different times during the $e^- + 1s$ collision: (a) $E_i = 25.0$ eV (below the $2s^2$ resonance energy); (b) $E_i = 31.6$ eV (close to the $2s^2$ resonance energy); (c) $E_i = 36.1$ eV (close to the $2s3s$ resonance energy).

wave packet with $w = 30$ a.u. and $E_i = 31.6$ eV. Thus, with a sufficiently narrow wave packet in energy space, one should be able to use the TDCC technique to map out the shape of a resonance.

One of the nice features of the time-dependent method is that it allows one to study the formation and decay of autoionizing states as a function of time. In Fig. 4, we show "snapshots" of the probability density $|\Psi(r_1, r_2, t)|^2$ near the origin, at different times during the collision. In this figure only, $t = 0$ is the time at the beginning of the iterations (i.e., $t_0 = 0$). In parts (a) of the figure, the incoming electron has an energy $E_i = 25.0$ eV, far below any resonance. As time evolves, the peak of the probability density centered originally at 110 a.u. moves toward the origin. The center of the packet arrives to the origin at $t = 83$ a.u., and then bounces back. At $t = 140$ a.u., the density is contained in the outgoing wave packet along the coordinate axes (elastic scattering). At this time, there is no trace of any $2s^2$ component, as expected from the very small dielectronic capture amplitude at this energy.

In parts (b) of the figure, the incoming electron has an energy $E_i = 31.6$ eV, close to the energy of the $2s^2$ resonance. In this case, the packet arrives at the origin at $t = 70$ a.u. A significant fraction of the total wave function is concentrated around the origin, and this is the part that is captured into the $2s^2$ state. As is seen in subsequent figures (b), the general shape of the total wave function near the origin is not changing with time, only decreasing in magnitude, as the doubly excited state decays.

A completely different picture is shown in Figs. 4(c), where the incoming electron has an energy close to the $2s3s$ resonance ($E_i = 36.1$ eV). The shape of the wave function is clearly changing in time, oscillating between the Φ_{2s3s} and the Φ_{2p^2} functions. An incident wave packet with an energy width of $\Delta E = 1.4$ eV cannot resolve the $2s3s$ and the $2p^2$ states (separated by 0.4 eV), and large-period oscillations are found in the dielectronic capture probabilities.

In conclusion, we have been able to carry out the first fully quantal time-dependent study of the dielectronic capture of an incident electron into a doubly excited state followed by autoionization. With the procedure we have outlined, the effects of numerical approximations can, in principle, be made arbitrarily small. The theoretical framework demonstrated here provides a basis for developing practical methods for treating resonances in the $(e, 2e)$ problem.

We would like to thank Dr. Francis Robicheaux for a number of helpful suggestions. This work was supported in part by the U.S. Department of Energy, and a subcontract from Los Alamos National Laboratory. Computational work was carried out at the National Energy Research Supercomputer Center in Oakland, CA.

[1] I. Bray and A. T. Stelbovics, Phys. Rev. Lett. **70**, 746 (1993).
[2] D. Kato and S. Watanabe, Phys. Rev. Lett. **74**, 2443 (1995).
[3] K. Bartschat and I. Bray, J. Phys. B **29**, L577 (1996).
[4] T. N. Rescigno, M. Baertschy, W. A. Isaacs, and C. W. McCurdy, Science **286**, 2474 (1999).
[5] J. P. van den Brink, J. van Eck, and H. G. M. Heideman, Phys. Rev. Lett. **61**, 2106 (1988).
[6] O. Samardzic, L. Campbell, M. J. Brunger, A. S. Kheifets, and E. Weigold, J. Phys. B **30**, 4383 (1997).
[7] D. H. Madison, V. D. Kravtsov, J. B. Dent, and M. Wilson, Phys. Rev. A **56**, 1983 (1997).
[8] C. W. McCurdy and T. N. Rescigno, Phys. Rev. A **62**, 032712 (2000).
[9] M. S. Pindzola and D. R. Schultz, Phys. Rev. A **53**, 1525 (1996).
[10] M. S. Pindzola and F. Robicheaux, Phys. Rev. A **54**, 2142 (1996).
[11] M. S. Pindzola and F. Robicheaux, Phys. Rev. A **55**, 4617 (1997).
[12] D. R. Schultz, C. Bottcher, D. H. Madison, J. L. Peacher, G. Buffington, M. S. Pindzola, T. W. Gorczyca, P. Gavras, and D. C. Griffin, Phys. Rev. A **50**, 1348 (1994).
[13] S. L. Haan, R. Grobe, and J. H. Eberly, Phys. Rev. A **50**, 378 (1994).
[14] W. Ihra, M. Draeger, G. Handke, and H. Friedrich, Phys. Rev. A **52**, 3752 (1995).
[15] A. K. Bhatia and A. Temkin, Phys. Rev. A **11**, 2018 (1975).
[16] J. S. Parker, L. R. Moore, K. J. Meharg, D. Dundas, and K. Taylor, J. Phys. B **34**, L69 (2001).
[17] U. Fano, Phys. Rev. **15**, 1866 (1961).